
This is the **accepted version** of the article:

Martin Martinez, Javier; Rodriguez, Rosana; Nafria, Montserrat; [et al.]. «An unsupervised and probabilistic approach to Pavlov's dog experiment with OxRAM devices». Microelectronic Engineering, Vol. 215 (July 2019), art. 111024. DOI 10.1016/j.mee.2019.111024

This version is available at <https://ddd.uab.cat/record/249285>

under the terms of the  license

An unsupervised and probabilistic approach to Pavlov's dog experiment with OxRAM devices

M. Pedro^{1*}, J. Martin-Martinez¹, R. Rodriguez¹, M.B. Gonzalez², F. Campabadal² and M. Nafria¹

¹*Departament d'Enginyeria Electrònica, Universitat Autònoma de Barcelona (UAB) Campus UAB. 08193 Bellaterra. Spain.*

²*Institut de Microelectrònica de Barcelona, IMB-CNM, CSIC. Campus UAB. 08193 Bellaterra. Spain.*

E-mail address of corresponding author: marta.pedro@uab.es

Abstract

In this work, a potential basis for implementing unsupervised associative learning in two or more memristors within neuromorphic architectures is proposed. The experimental demonstration is carried out by means of emulating the Pavlov's dog classical conditioning experiment with two OxRAM devices, in which the dependence of the probability of association on test parameters, such as the pulse amplitude, is studied.

Keywords: Associative learning, Memristors, Neuromorphic, OxRAM, Unsupervised Learning

1. Introduction

Memristors are being widely investigated for their application as synaptic devices in neuromorphic architectures. Their characteristics allow merging computation and memory, which is of great interest when a bio-inspired approach is considered. With this purpose, learning models coming from psychobiology are being demonstrated concerning the programmable conductance that these devices present, which is identified as the synaptic weight. The ability of fine-tuning their conductivity state according to the features of the past electrical activity demonstrates their plasticity property. Unsupervised learning rules, which rely on the dependences of plasticity on time or frequency correlations between the pre and post-synaptic activities, have been already proven in single electronic devices in a large variety of memristive technologies [1-4]. However, there is still a lack of understanding on how bio-inspired local learning rules should be designed when the interaction between two or more memristors is considered. In the biological brain, complex cognitive processes arise from associative learning mechanisms, involving the causal interaction between multiple neuronal layers, and thus, of a large amount of synapses. The study of associative learning between electronic synapses would suppose a step towards the implementation of neuromorphic associative memories and hierarchical computing networks, able to store and recall symbolic knowledge, as occurs in the mammalian neural system.

A simple case of associative learning can be found in the classical conditioning experiments initially conducted by I. Pavlov [5]. In classical conditioning, two stimuli are considered: one is the so-called unconditioned stimulus (US), and the second is the neutral stimulus (NS). The US triggers a response of the system, labelled as the unconditioned response (UR). On the other hand, the NS does not provoke the UR. It is through a stage of conditioning in which the NS is associated to US, so that the NS becomes a conditioned stimulus (CS), generating a system response similar to the UR. The experiment that Pavlov carried out was actually with dogs: the US was the sight of food, which made the dogs salivate (UR). The NS he employed was the ringing of a bell, which was neutral to the dogs in the sense that, only with its presence no salivation was induced. Pavlov discovered that, by consecutively ringing the bell when feeding the dogs, they would start responding similarly to both US (food) and NS (ringing of the bell), the latter becoming a CS. That is, they would salivate when hearing the bell without the presence of food, because the dogs associated it with their feeding time. This finding had great implications, being today the basis of the associative learning theory.

Electronic emulations of classical conditioning and Pavlov's dog test have actually been carried out with memristive devices, either using a single partially-volatile device [6], a single non-volatile device [7, 8], or a pair of volatile organic transistors with discrete CMOS neurons, being the latter focused on the implementation of a short-term associative memory [9]. In our work, we introduce an unsupervised electronic setup for studying a basic process of associative learning, involving the use of a pair of non-volatile OxRAM devices and being the test scheme analogous to the original Pavlov's dog experiment. Moreover, we propose to analyze the conditioning efficiency by establishing a probabilistic association criterion. This is motivated by, on the one hand, taking into account the device-level variability found in memristive technologies such as OxRAM, which is often considered as an issue. On the other hand, significant variability is also found in biological neural and synaptic populations, as well as in their plasticity property, yet this variability is thought to be a typical (and maybe necessary) feature for a healthy nervous system [10-12]. This is the main reason for which statistical methods and models have been successfully incorporated to the computational neuroscience research during the last decades [13]. Therefore, it is plausible to design probabilistic learning rules for their application in neuromorphic architectures considering the variability observed in the devices to be employed.

2. Materials and methods

2.1. Tested samples and setup description

The tested RRAM devices consist of $5 \times 5 \mu\text{m}^2$ TiN-Ti-HfO₂-W Metal-Insulator-Metal (MIM) structures. Details of their fabrication can be found in [14]. An example of their I-V characteristics is shown in Figure 1, in which bipolar resistive switching phenomena can be observed.

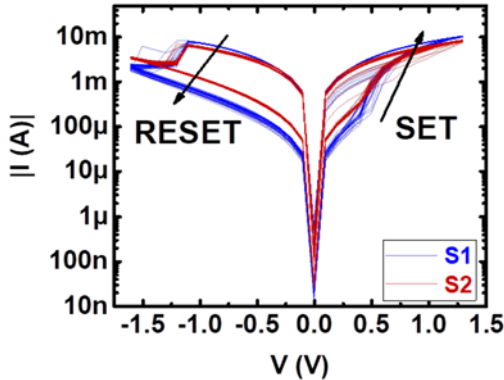


Figure 1. Examples of I-V characteristics of the tested samples, S1 (blue) and S2 (red). Resistive switching is described by two main processes: the SET process, which is the transition from a high resistance state to a lower one, and the RESET, which is the reverse behavior. Both samples present similar SET and RESET voltages.

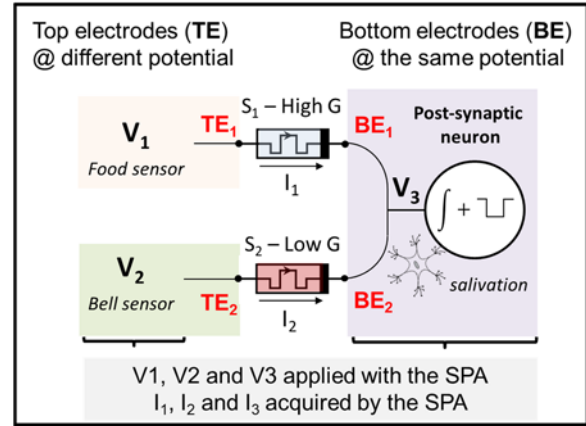


Figure 2. Scheme of the experimental setup for the electronic Pavlov's dog experiment. V_1 and V_2 are the input signals of the system, connected to the post-synaptic neuron via two Oram devices, S_1 and S_2 . Initial conditions for the two samples are also displayed, being S_1 at a high conductivity state, whereas S_2 has a low conductivity state.

The scheme of the employed characterization setup for implementing associative learning is shown in Figure 2, involving a four-point manual probe station and a semiconductor parameter analyzer controlled via GPIB. In Figure 2, two RRAM devices represent the synaptic connection (S_1 , S_2) between two pre-synaptic sensors and a post-synaptic neuron (POST), which S_1 and S_2 have in common. The signals coming from the sensors are identified as V_1 and V_2 , which are the inputs of the system, and share the same amplitude value, V_d . On the other hand, V_3 represents the feedback signal triggered by the POST, and provides also a way to measure the response of the system. All of the employed signals are applied with a semiconductor parameter analyzer (SPA) Agilent 4156C. The smart control of the SPA is employed for emulating the POST as an integrate-and-fire neuron. The current flowing through S_1 and S_2 is collected by the SPA, and the amount of charge that the neuron is receiving is computed and accumulated over time. When the accumulated charge reaches a defined threshold Q_{thr} , the virtually stored charge is cleared, and the POST neuron fires a voltage pulse towards S_1 and S_2 , with amplitude $V_3 = -V_d$ and a determined pulse-width PW. Since this post-synaptic pulse represents a response to the pre-synaptic activity, two different situations can occur for each of the synapses: a voltage drop of $2V_d$ if there is some pre-synaptic activity coming from the sensor, or a voltage drop of $-V_d$ if there is no pre-synaptic signal.

2.2. Test scheme

The electrical classical conditioning scheme that we propose consists in emulating the Pavlov's dog test. The goal is to associate the V_1 and V_2 inputs through experience, so that the activation of the POST (salivation) is achieved not only with the presence of V_1 (food), but also with the single application of V_2 (bell ringing). This is because during the trials V_2 appears paired with V_1 , so an associative process between the inputs takes place. Initially, S_1 has a high conductivity level, since the dog salivation is related to the sight of food, whereas S_2 has a low conductivity, because the ringing of the bell is assumed to not cause salivation. The whole learning sequence is represented in Figure 3. The voltage drops at S_1 (V_{S1} in Figure 3.a) and S_2 (V_{S2} in Figure 3.b), which are defined as $V_{S1} = V_1 - V_3$ and $V_{S2} = V_2 - V_3$, are plotted over time. Next, the V_1 (US) and V_2 (NS \rightarrow CS) waveforms (Figure 3.c and Figure 3.e, respectively) are plotted over time. The neuron response $|V_3|$ is also depicted in Figure 3.g, symbolizing the dogs' salivation. The currents through S_1 (I_1 in Figure 3.d) and S_2 (I_2 in Figure 3.f) which were measured during one of the tests are also shown as an example, which were recorded only when the POST was firing a pulse, in order to speed the performance of the tests.

First of all, a current-controlled forming process is performed on the S_1 and S_2 devices, which are located within the same dice. Next, five compliance-free RESET and SET processes are induced to each of the samples (not shown in Figure 3), in order to set their conductivity states within a certain range, following the procedure of the previous works [A-B]. The maximum voltage applied to the sample with the S_1 role was of $V_{set} = 2V_d$, whereas in the case of S_2 , it was of $V_{set} = V_d$. In this way, the conductivity state of S_1 was set to a high value ($G > 30G_0$), whereas S_2 was set to a low value ($G \leq 5G_0$). The learning sequence starts with the single application of $V_1 = V_d$.

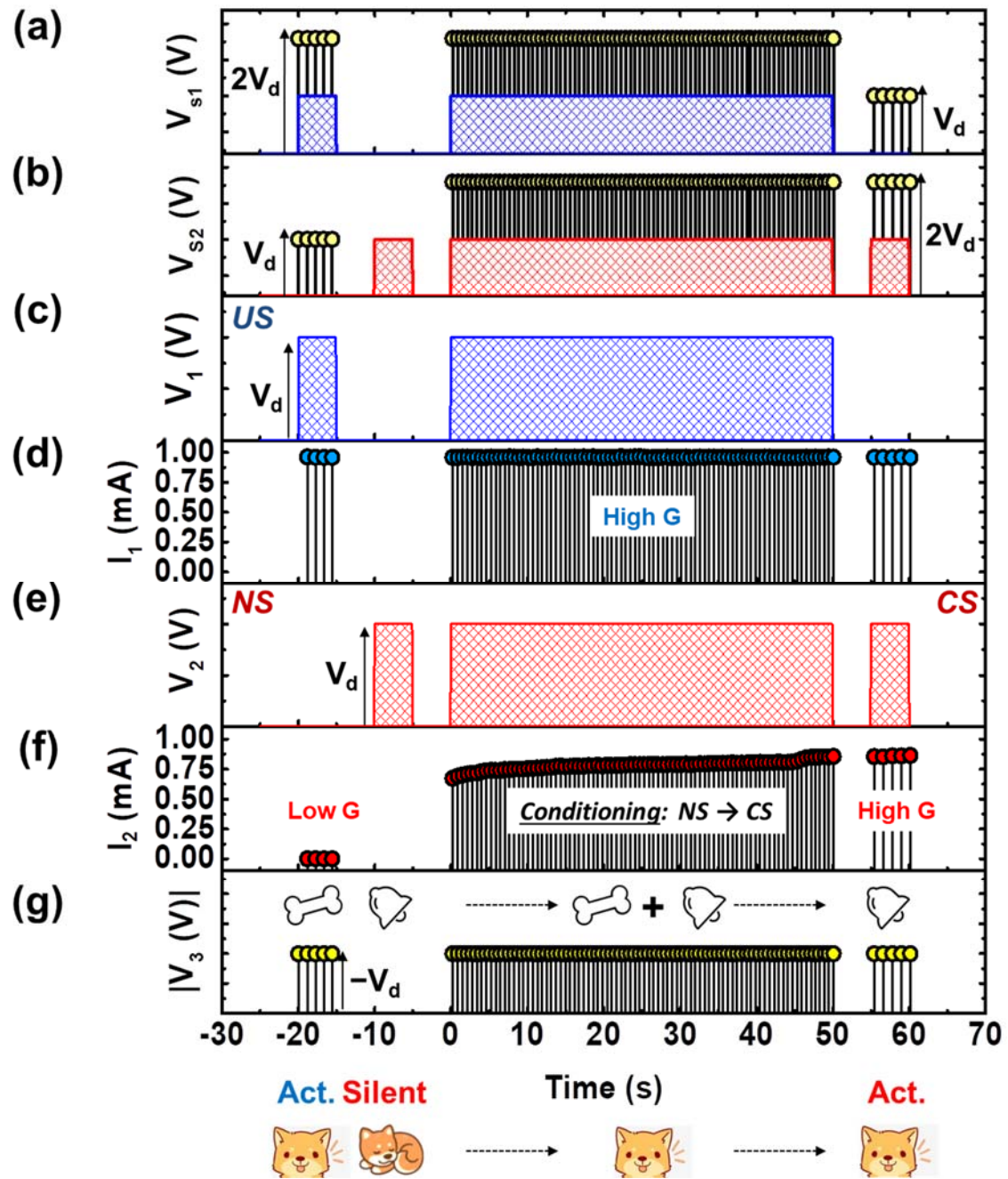


Figure 3. Particular case of voltage and intensity evolutions over a learning sequence where the association process took place. The bottom part of the figure shows an analogy between the POST activity and the Pavlov dog's behavior. **(a)** Voltage drop at S1, defined as $V_{s1} = V_1 - V_3$. **(b)** Voltage drop at S2, defined as $V_{s2} = V_2 - V_3$. **(c)** Voltage waveform V_1 corresponding to the US, given by sensor 1. Its high level is of V_d . **(d)** Intensity flowing through S1, measured only when the POST triggered a spike. The conductivity state of S_1 is also indicated in G_0 units, being of $35.36G_0$, corresponding to a high conductivity state. **(e)** Voltage waveform V_2 with a high level of V_d . V_2 corresponds to the NS, given by sensor 2, which after the conditioning stage becomes CS if the association process has occurred. **(f)** Intensity flowing through S2, measured only when the POST triggered a spike. The conductivity state of S2 is also indicated in G_0 units, being of $0.063G_0$ before the conditioning stage, and of $31.67G_0$ after the association process, corresponding to low and high conductivity states, respectively. **(g)** Voltage waveform $|V_3|$ corresponding to the POST activity, given as spikes with amplitude $-V_d$. In this case, the POST responds first only to the presence of V_1 , whereas after the association process, it also responds to V_2 .

($-20s < t < -15s$), and then of $V_2 = V_d$ ($-10s < t < -5s$). The POST responds to V_1 because S1 presents a high conductivity state from the beginning of the test. On the other hand, no firing is expected to occur when only $V_2 = V_d$ is applied, since it represents the NS, and S2 has a very low conductivity. Next, both V_1 and V_2 are active together during a training time of $t_{tr} = 50s$. Because of the current through S1 is high, eventually, the accumulated charge in POST reaches Q_{thr} , so that it fires a voltage pulse as a response. The voltage drop at S2, which has a magnitude of $2V_d$, causes S2 to increase its conductivity. This event may occur multiple times during this phase, as shown in Figure 3. The value of V_d has to be carefully chosen as to induce a positive

change in S2 conductivity only when V_2 and the neuron pulses are overlapping. That is, the voltage drop at S2 of $2V_d$ has to be large enough to induce a SET process, but a voltage drop of magnitude V_d in device S2 should not. On the other hand, the conductivity state of S1 remains constant during the whole test, since a voltage drop of $2V_d$ is not large enough as to increase its conductivity state above its initial value, which is already large. This stage with paired V_1 and V_2 is the core of the classical conditioning experiment, because it is when associative learning, which implies a change in S2 conductivity when V_1 and V_2 are active simultaneously, occurs. However, this does not mean that necessarily V_2 and the POST will be fully connected in a single learning phase, with S2 presenting a conductivity level similar to the one of S1. Different levels of association might be achieved over time by playing with the test conditions, such as V_d , since S2 can display many conductivity levels.

Finally, $V_2=V_d$ is applied as a single input ($55s < t < 60s$), and the current through S2 is high enough to trigger the POST response, which is similar to the response evoked by single V_1 application, so V_2 has been effectively associated to V_1 . In this work, we tested different V_d , ranging from 0.2V up to 0.4V, while keeping the rest of test parameters fixed: $Q_{thr}=0.1mC$ and $PW=0.1ms$.

3. Results and Discussion

The relative conductivity change $\Delta g_2(t)$ of S2 during the conditioning stage is defined as the difference between the measured conductivity $g_2(t)$, and the conductivity before the conditioning stage, g_{NC} . In Figure 4, a few examples of the evolution over time of the relative conductivity change normalized to g_{NC} ($\Delta g_2(t)/g_{NC}$) measured on the same device are depicted. Each color represents a different value of the employed V_d . Despite of using the same test parameters, different $\Delta g_2(t)$ waveforms are observed during the trials due to device-level variability.

In order to study the effects of the test parameters on the association process, the cumulative distribution functions (cdf) of the conductivity values observed after conditioning, $g_{CC}=\Delta g_2(t=55s)$, are shown in Figure 5, where each cdf corresponds to a different V_d . Results in Figure 4 and 5 show that the associative process has a dependence with the employed V_d . As to provide a probabilistic interpretation of the conditioning efficiency, an association criterion in terms of a conductivity ratio threshold (CCR_{th}) is defined, assuming that if the conditioning conductivity ratio $CCR=g_{CC}/g_{NC}$ is larger or equal than the CCR_{th} ($CCR \geq CCR_{th}$), the conditioning stage has been effective.

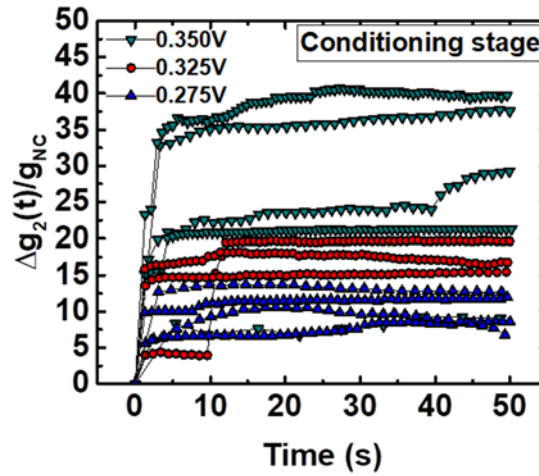


Figure 4. $\Delta g_2(t)/g_{NC}$ examples for different V_d levels during the conditioning stage. Each curve is related to the I_2 values measured when POST was firing a pulse for different V_d values, performed on the same device.

In Figure 5, three criteria are marked: $CCR_{th}=0.1$, $CCR_{th}=1$ and $CCR_{th}=10$. The probability of association is computed as the number of trials where a particular association criterion CCR_{th} is met, corresponding to the number of trials in which the CCR is above CCR_{th} , and corresponds to:

$$Probability\ of\ association = 1 - P(CCR < CCR_{th})$$

The probabilities of association as a function of the tested V_d values are depicted in Figure 6. It can be observed that the probability of association increases with increasing V_d , up to the maxima $V_d=0.325V$. Above this value, any association process can take place: the voltage drop of V_d , originated when V_2 is active before the training stage ($-10s < t < -5s$) is large enough to evoke a SET process to S2 on its own, being its conductivity state increased in the wrong scenario.

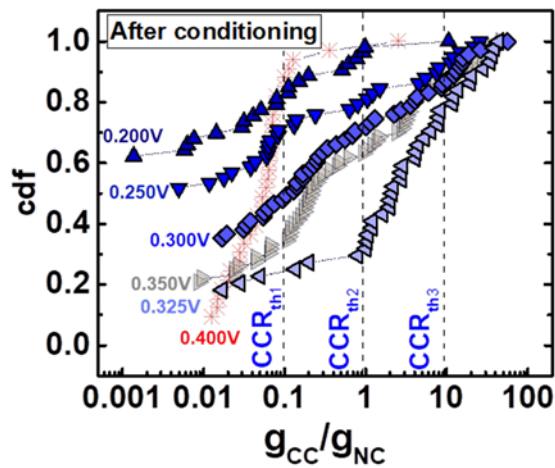


Figure 5. Cdfs of the relative conductivity change achieved after the conditioning stage, g_{CC}/g_{NC} , for different V_d . The associative process requires a proper choice of V_d . Three association criteria examples are depicted: $CCR_{th1}=0.1$, $CCR_{th2}=1$ and $CCR_{th3}=10$. Interpretation of these data is given in Figure 6.

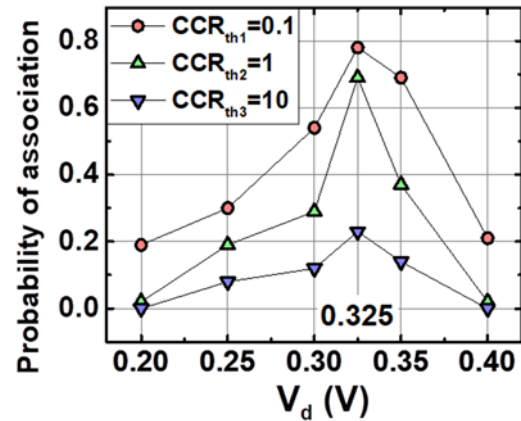


Figure 6. The association probability for three different criteria of association ($CCR_{th} = 0.1, 1$ and 10) is represented as a function of V_d . Probability increases with increasing V_d up to a limit where no association process takes place, since S2 conductivity changes before any pairing between V1 and V2 is made. Maxima are found at $V_d=0.325V$.

4. Conclusions

An associative memory presents the ability to learn and recall the relationship between unrelated items, being the interaction between neurons and the synaptic plasticity their basis. Animal-beings are able to develop non-instinctive behaviors and establish symbolic relationships between facts or events through learning processes such as classical conditioning, observed by I. Pavlov and his dogs. Taking advantage of the synaptic plasticity property of memristive devices, the study of fundamental associative learning rules would suppose a step towards the implementation of neuromorphic associative memories and hierarchical computing networks. In this work, an electronic version of the Pavlov's dog experiment to be employed in two or more memristive devices is proposed, as a possible basis for implementing unsupervised associative learning within neuromorphic architectures. The experiments show that the probability of having the post-synaptic neuron responding to the neutral stimulus when it is the only active input is highly increased after the conditioning stage, in analogy to Pavlov's dog behavior. Because of device-level variability, an association criterion has to be defined. We tested the association probability dependence on the amplitude of the employed voltage waveforms, and found that the association level reached during conditioning increases with this parameter, up to a certain value, for which any association learning process cannot occur.

References

- [1] S.H Jo et al. Nanoscale memristor device as synapse in neuromorphic systems. *Nano Lett.* 10, 4 (2010) 1297-1301. <https://doi.org/10.1021/nl904092h>
- [2] T.Serrano-Gotarredona et al. STDP and STDP variations with memristors for spiking neuromorphic learning systems. *Front Neurosci.* 7 (2013): 2. <https://doi.org/10.3389/fnins.2013.00002>
- [3] M.Prezioso et al. Self-Adaptive Spike-Time-Dependent Plasticity of Metal-Oxide Memristors. *Sci Rep* 6 (2016): 21331. <https://doi.org/10.1038/srep21331>
- [4] Z.Yide et al. Implementation of memristive neural networks with spike-rate-dependent plasticity synapses. *IEEE IJCNN* (2014): 2226-2233. <https://doi.org/10.1109/IJCNN.2014.6889740>
- [5] A.H. Klopff. A neuronal model of classical conditioning. *Psychobiology*, 16.2 (1988): 85-125. <https://doi.org/10.3758/BF03333113>
- [6] Z-H. Tan et al. Pavlovian conditioning demonstrated with neuromorphic memristive devices. *Sci Rep* 7.1 (2017): 713. <https://doi.org/10.1038/s41598-017-00849-7>
- [7] M. Ziegler et al. An Electronic Version of Pavlov's Dog. *Adv Funct Mater* 22.13 (2012): 2744-2749. <https://doi.org/10.1002/adfm.201200244>
- [8] C. Wu et al. Mimicking classical conditioning based on a single flexible memristor. *Adv Mater* 29(10) (2017): 1602890. <https://doi.org/10.1002/adma.201602890>
- [9] O. Bichler et al. Pavlov's dog associative learning demonstrated on synaptic-like organic transistors. *Neural Comput* 25.2 (2013): 549-566. https://doi.org/10.1162/NECO_a_00377
- [10] E. Marder. Variability, compensation, and modulation in neurons and circuits. *PNAS* 108. Supplement 3 (2011): 15542-15548. <https://doi.org/10.1073/pnas.1010674108>
- [11] D. Parker. Synaptic Variability Introduces State-Dependent Modulation of Excitatory Spinal Cord Synapses. *Neural Plast.* 2015; 2015: 512156. <https://doi.org/10.1155/2015/512156>

- [12] A. Neishabouri and A.A. Faisal. Axonal Noise as a Source of Synaptic Variability. *PLoS Comput Bio* 10.5 (2014): e1003615. <https://doi.org/10.1371/journal.pcbi.1003615>
- [13] MD. McDonnell et al. Neuronal stochastic variability: influences on spiking dynamics and network activity. *Front Comput Neurosci* 10 (2016): 38. <https://doi.org/10.3389/fncom.2016.00038>
- [14] S. Poblador et al. Investigation of the multilevel capability of TiN/Ti/HfO₂/W resistive switching devices by sweep and pulse programming. *Microelectron Eng* 187-188 (2018): 148-153. <https://doi.org/10.1016/j.mee.2017.11.007>
- [15] M. Pedro et al. A Flexible Characterization Methodology of RRAM: Application to the Modeling of the Conductivity Changes as Synaptic Weight Updates. *Solid-State Electron Special Issue of EUROSOI-ULIS 2018 Accepted* (2019).
- [16] M. Pedro et al. Tuning the conductivity of resistive switching devices for electronic synapses. *Microelectron Eng Special Issue of INFOS 2017*, 178, 89-92. <https://doi.org/10.1016/j.mee.2017.04.040>

Acknowledgements

This work has been partially supported by the Spanish MINECO and ERDF (TEC2016-75151-C3-1-R, TEC2013-45638-C3-1-R and TEC2017-84321-C4-1-R), and it has made use of the Spanish ICTS Network MICRONANOFABS.

